



New dimensionless equation for mass transfer at evaporation of open liquid surface in mixed or forced convection

Evelin VARJU^{a,*}, Tibor POÓS^b

^a Department of Building Services and Process Engineering, Faculty of Mechanical Engineering, Budapest University of Technology and Economics, Műgyetem rkp. 3., H-1111 Budapest, Hungary

^b Department of Building Services and Process Engineering, Faculty of Mechanical Engineering, Budapest University of Technology and Economics, Hungary

ARTICLE INFO

Keywords:

Forced convection
Mixed convection
Sherwood equation
Cases of evaporation
Equivalent characteristic length

ABSTRACT

The process of evaporation can be grouped into 48 different cases depending on the conditions and properties of the gas and liquid. The publications found in the literature and the correlations specifying the evaporation rate can be classified into these cases. A new dimensionless equation was created that gives the value of the evaporation rate in the case of evaporation with steady-state gas and liquid conditions under mixed or forced convection. To create the equation, we used our own measurement results, as well as the measurement results found in the literature, which were published with appropriate data. During the comparison with equations found in the literature, the new dimensionless equation best approximated the measurement results with an average relative error of 12.4 %.

1. Introduction

During evaporation, the thin gas layer above the liquid surface becomes saturated with the vapor of the liquid as a result of molecular diffusion. From the thin gas layer, the vapor moves to the bulk gas in two ways: diffusion and convection (Stefan flow). Most researchers consider only two phenomena in this case, the evaporation under natural or forced convection. Several researchers [2–6] found that up to a certain gas velocity, the diffusion process resulting from the difference in temperature and humidity is the determining factor, rather than the forced movement caused by the air flow. To distinguish between the two evaporation phenomena according to the air velocity value, values between $v_G = 0.1 - 0.15 \text{ m/s}$ can be found in the literature [7–9]. However, this distinction does not take into account the evaporation under mixed convection. During mixed convection the effects of the buoyancy force resulting from the density difference and the forced movement resulting from the gas velocity are of the same magnitude [2], so they must be taken into account together. The Ri number [10] – the quotient of the Gr number and the square of the Re number – and the Fr number [11] – the quotient of the cube of the air speed and the buoyant force projected onto the diffusion path length – are available to distinguish the individual convection cases.

The evaporation rate is influenced by the conditions and properties

of the gas and liquid. These include the properties of the gas, temperature, humidity, characteristic velocity, turbulence intensity of the gas and total pressure of the gas above the liquid surface; as well as the properties of the liquid, its surface temperature, convection and the size of the liquid surface.

In the case of evaporation under forced convection, Dalton [12] established for the first time that the intensity of evaporation is proportional to the partial vapor pressure difference between the liquid surface and the bulk gas, as well as the velocity of the air flow. Later, researchers established that there is a power relationship between the two factors [1,2,10,13–17]:

$$N = (a + bv_G)(p_v^f - p_v^G)^n \quad (1)$$

In the equation of the evaporation rate, the exponent (n) of the partial vapor pressure difference can be specified with a given numerical value, depending on the air velocity [1,2,10,14], or also with a logarithmic expression [18]. Especially for outdoor measurements, the location of the air velocity measurement in both vertical and horizontal directions is even more important than with natural convection [19]. In the literature on the evaporation of lakes, the air velocity was measured at different heights, but most often measurements were made at a height of $\sim 2 \text{ m}$ from the water surface. Thus, in order to be able to determine the evaporation rate with the given correlation, we have to measure the air velocity also at that height. Measurement results at a different height

* Corresponding author.

E-mail addresses: varju.evelin@gpk.bme.hu (E. VARJU), poos.tibor@gpk.bme.hu (T. POÓS).

<https://doi.org/10.1016/j.ijheatmasstransfer.2024.125522>

Received 17 November 2023; Received in revised form 28 March 2024; Accepted 29 March 2024

Available online 11 April 2024

0017-9310/© 2024 The Author(s). Published by Elsevier Ltd. This is an open access article under the CC BY-NC-ND license (<http://creativecommons.org/licenses/by-nc-nd/4.0/>).

Nomenclature			
A	surface [m^2]	y	mass fraction [$kg_{moisture} / kg_{wet\ gas}$]
c	molar concentration [mol / m^3]	Y	absolute humidity of gas [$kg_{moisture} / kg_{dry\ gas}$]
D	diffusion coefficient [m / s]	<i>Greek Letters</i>	
Fr	Froude number [1]	δ	relative error
g	gravitational acceleration [m / s^2]	μ	dynamic viscosity [$Pa \cdot s$]
Gr	Grashof number for mass transfer [1]	ρ	density [kg / m^3]
Gu	Guckman number [1]	ν	kinematic viscosity [m^2 / s]
h	step distance [1]	φ	relative humidity [1]
k	mass transfer coefficient [m / s]	Φ_T	temperature correction term [1]
L	characteristic length [m]	Φ_p	vapour pressure correction term [1]
\dot{m}	mass flow rate [kg / s]	ω	point [1]
M	molar mass [$kg / kmol$]	<i>Subscripts and Superscripts</i>	
MAE	mean absolute error [1]	a, b, n	superscripts in Eq. (1)
N	evaporation rate [$kg / (m^2 s)$]	$A \dots F$	superscripts in Eq. (3)
p	pressure [Pa]	c	molar value
r	latent heat of evaporation [J / kg]	e	equivalent
R	ideal gas constant [$8.314 J / (mol^\circ C)$]	$evap$	evaporating
R^2	coefficient of determination [1]	f	liquid surface temperature
$RMSE$	root mean square error [1]	G	bulk gas or bulk gas temperature
Ra	Rayleigh number for mass transfer [1]	i	running number
Re	Reynolds number [1]	j	upper limit
Ri	Richardson number [1]	L	liquid
Sh	Sherwood number [1]	max	maximum value
Sc	Schmidt number [1]	$meas$	measured value
T	temperature [$^\circ C$]	min	minimum value
v	velocity [m / s]	$pred$	predicted value
x	salt concentration [ppm]	tot	total gas
		v	liquid vapor

must be converted to the required height with a correlation suitable for specifying an air velocity profile [20,21].

In the area of mass transfer, the Sh number is suitable for determining the mass transfer coefficient. In the case of mass transfer under forced or mixed convection, the Re and Sc numbers are primarily used in addition to the Sh number. This type of correlation will henceforth be called Sherwood equation:

$$Sh = ARe^B Sc^C \quad (2)$$

The advantage of using dimensionless correlations is that they can be considered a general equation, as they include the temperature dependence of the material characteristics and the characteristic size.

At low air velocities, the liquid surface has a flat surface, however, at higher air velocities, ripples or waves may appear on the surface, while at a certain air flow, droplet entrapment may also occur, which must be taken into account when determining the evaporation rate. With the formation of waves, the intensity of evaporation increases, but not only because of the surface increase, but also because of the changed flow conditions [22].

Among the gas condition that also affect the evaporation rate is the ambient pressure. Several researchers found that the evaporation rate increases with a decrease in pressure, for example with an increase in altitude [23,24].

Most of the experiments in the literature examined the evaporation of one of the most important liquids: water. However, there were also studies of the evaporation of other, mainly volatile, liquids [15,22, 25–27], thereby examining the effect of the properties of the liquid in terms of evaporation rate.

Temperatures that affect the rate of evaporation include the bulk temperature of the gas and the temperature of the liquid surface. If conductive heat transfer does not occur with the evaporating liquid,

then after a sufficiently long time a state of equilibrium is reached during evaporation. In case of sufficiently high air velocity ($v_G > \sim 3 m/s$), the surface temperature of the liquid will keep to the wet bulb temperature [28,29]. The surface temperature of the liquid can be changed by applying different heating methods in order to examine the phenomenon of evaporation in a wider temperature range [2,30].

Some researchers [20,23–25,31–33] believed that the correlations created from laboratory measurements are not suitable for describing the evaporation rate of larger water surfaces (e.g. reservoirs, lakes, rivers). The evaporation rate will be lower with a larger liquid surface, since the humidity of the gas flowing over the evaporating surface increases along the direction of flow, that is, a ‘vapor layer’ is formed, which reduces the driving force of mass transfer. To take this effect into account, a pan coefficient [34,35], liquid surface size or liquid surface characteristic length were displayed in the equation of the evaporation rate [11,36–41].

There are different correlations in the literature, depending on what parameter has been used to make the estimation of the evaporation rate even more accurate.

Table 1 shows the correlations collected from the literature for evaporation rate in mixed and forced convection for the evaporation under steady-state conditions.

The main deficiency in the publications was caused by the fact that the values of the operating parameters set during the measurement and the results were reported incompletely or incorrectly. The correlation created on the basis of the measurement results can only be used to calculate the evaporation rate if it is known under what conditions the equation was created and what are the validity ranges bound to its use. In many cases, these are not provided or are incomplete, so its use and the results obtained with it become questionable. In addition, specifying the measurement conditions as a range is not a sufficient condition for

Table 1

Correlations for evaporation rate in mixed and forced convection under steady-state conditions.

Ref.	Name	Equation in SI
[13]	Himus and Hinchley	$N = 10^{-8}(6.459 + 2.813v_G)(p_v^f - p_v^G)$
[18,43]	Thiesenhusen	$N = 0.0081\sqrt{v_G}\ln\left(\frac{p_{tot} - p_v^G}{p_{tot} - p_v^f}\right)$
[28]	Lurie and Michailoff	$N = 10^{-8}(4.58 + 3.5v_G)(p_v^f - p_v^G)$
[14]	Leven	$N = 8.68 \cdot 10^{-6} v_G^{0.727} \left(\frac{p_v^f - p_v^G}{133.322}\right)^{\frac{1.06}{v_G^{0.0567}}}$
[22]	Smolsky and Sergeyev	$Sh = 0.094Re^{0.8}Sc^{0.33}Gu^{0.2}$
[44]/a	Yen and Landvatter	$Sh = 12.7 + 0.00288Re$
[44]/b	Yen and Landvatter	$N = (0.054 + 0.1v_G^{1.52})\frac{(p_v^f - p_v^G)}{r_L}$
[45]	Baturin	$N = 10^{-8}(1.31 + 2.92v_G)(p_v^f - p_v^G)$
[46]	Bennett and Myers	$Sh = 0.66Re^{0.5}Sc^{1/3}$
[47]	Chuck and Sparrow	$Sh_h = 0.047Re_h^{0.711} / \left(\frac{L}{h}\right)^{0.0968}$
[36]	Haji and Chow	$N = 0.0359Sc^{-0.4}\ln\left(1 + \frac{y_f - y_G}{1 - y_f}\right)\left(\frac{\dot{m}_G}{A_G}\frac{\rho_G^f}{\rho_G^G}\right)^{0.8}\left(\frac{\mu_G}{L}\right)^{0.2}$
[48]	Sartori	$N = 2.664 \cdot 10^{-3} v_G^{0.5} \frac{p_v^f - p_v^G}{p_{tot}}$
[15]/a	Braun and Caplan	$N = 2.577 \cdot 10^{-9} M_L (p_v^f - p_v^G) v_G^{0.625}$
[15]/b	Braun and Caplan	$N = 3.251 \cdot 10^{-9} M_L^{1.08} (p_v^f - p_v^G)^{0.98}$
[15]/c	Braun and Caplan	$N = 1.216 \cdot 10^{-8} M_L (p_v^f - p_v^G)^{0.89} v_G^{0.56}$
[15]/d	Braun and Caplan	$N = 9.065 \cdot 10^{-10} M_L (p_v^f - p_v^G)^{1.2}$
[49,50]	Rotkegel	$Sh = 0.0279Re^{0.791}Sc^{0.44}$
[39]	Hummel et al.	$N = 2.761 \cdot 10^{-6} M_L^{0.833} (p_v^f - p_v^G) \cdot \left(\frac{1}{M_L} + \frac{1}{M_G}\right)^{0.25} \frac{1}{(T_L^f + 273.15)^{0.05}} \sqrt{\frac{v_G}{Lp_{tot}}}$
[10]/a	Pauken	$N = 10^{-6}(20.56 + 27.21v_G + 6.92v_G^2) \cdot (10^{-3}(p_v^f - p_v^G))^{(1.22 - 0.19v_G + 0.038v_G^2)}$
[10]/b	Pauken	$Sh = 0.14Ra^{0.33} \cdot (1 + 0.543 - 0.408\left(\ln\left(\frac{Gr}{Re^2}\right)\right) + 0.0826\left(\ln\left(\frac{Gr}{Re^2}\right)\right)^2)$
[30]/a	Al-Shammiri	$N = 6.092 \cdot 10^{-6} v_G^{1.058} x^{-0.16} (p_v^f - p_v^G)^{0.376}$
[30]/b	Al-Shammiri	$N = 5.124 \cdot 10^{-7} v_G^{1.478} x^{-0.103} (p_v^f - p_v^G)^{0.654}$
[1]/a	Moghiman and Jodat	$N = 10^{-8}(0.0106 + 3.77v_G) \cdot (p_v^f - p_v^G)^{(-1.255v_G^3 + 2.182v_G^2 - 1.362v_G + 1.377)}$
[1]/b	Moghiman and Jodat	$Sh = 0.14Ra^{\frac{1}{3}} \left[1 + \left(\frac{0.036Re^{0.8}Sc^{1/3}}{0.14Ra^{1/3}}\right)^{1.075}\right]^{1/1.075}$
[2]/a	Jodat et al.	$N = 2.778 \cdot 10^{-7} (0.03262v_G^3 + 0.01814v_G^2 + 0.04818v_G + 0.02264) (p_v^f - p_v^G)^{(0.009v_G^2 - 0.132v_G + 1.186)}$
[2]/b	Jodat et al.	$Sh = 0.14Ra^{0.33} \cdot (1.441 - 0.345\ln\left(\frac{Gr}{Re^2}\right) + 0.22\left(\ln\left(\frac{Gr}{Re^2}\right)\right)^2 - 0.037\left(\ln\left(\frac{Gr}{Re^2}\right)\right)^3)$
[51]	Yanagi et al.	$N = 0.01\bar{\rho}_G v_G^{0.6} \left(\frac{0.622p_v^f}{p_{tot} - 0.378p_v^f} - \frac{0.622p_v^G}{p_{tot} - 0.378p_v^G}\right)$
[26]	Heymes et al.	$Sh = 0.145Re^{0.69}Sc^{0.87}$
[52]/a	Raimundo et al.	$N = 10^{-9}(37.17 + 32.19v_G)(p_v^f - p_v^G)$
[52]/b	Raimundo et al.	$N = 10^{-6}(22.77 + 215.85v_G - 23.59\varphi - 219.05\varphi v_G + 13.95\varphi v_G(T_L^f - T_G^G))$
[53]	Inan and Atayilmaz	$N = (0.28 + 0.784v_G) \frac{(p_v^f - p_v^G)^{0.695}}{r_L}$

Notification: T_L^f is the liquid surface temperature, v_G is the gas velocity, T_G^G is the gas temperature, φ is the relative humidity of gas, p_v^f is the partial pressure of liquid-vapour in the gas at the liquid surface temperature, p_v^G is the partial pressure of liquid-vapour in the gas at the gas temperature, Δp_v is the partial pressure difference of liquid-vapour between the bulk gas and liquid surface, L is characteristic length.

the reproducibility of the results, since specifying an insufficient number of conditions can be misleading and can lead to inaccurate results for many combinations of parameters.

In our previous work [42], we investigated evaporation under natural convection and created an equation for calculation of the

evaporation rate. With the established equation, the value of the evaporation rate can be determined for the evaporation case with the steady-state gas and liquid conditions in the range of $1.15 \cdot 10^5 \leq Ra \leq 1.13 \cdot 10^8$. The new equation was compared with the correlations in the literature, which gave the smallest deviation in the studied range with a

relative error of 9.5 %.

The current publication is a continuation of our previous work [42], but for evaporation with steady-state conditions under mixed or forced convection. None of the researches really took as a basis other effects or characteristics influencing the rate of evaporation, on the basis of which the evaporation cases could be grouped, apart from the nature of the gas flow. Among the many correlations found in the literature for determining the evaporation rate, there is no one that would be accepted by most researchers in case of wide application. Thus, the goal of our research was to create an equation describing the evaporation rate with steady-state gas and liquid conditions. The new equation describing the evaporation rate was compared with the correlations found in the literature.

2. Methods

Publications dealing with the phenomenon of evaporation can be grouped according to different aspects [54]. However, it enables a more differentiated and independent division if the grouping is done according to the similarity or difference of the factors that fundamentally influence the phenomenon. Thus, different evaporation cases were categorized based on the knowledge of gas (gas temperature and humidity) and liquid (liquid temperature) conditions [54]. Within the evaporation under forced or mixed convection, we distinguished cases where the gas and liquid conditions are steady-state, time-varying, locally-varying along the surface, or time- and locally-varying along the surface. In the course of our work, we dealt with the case of evaporation with steady-state gas and liquid conditions.

A case with steady-state gas conditions is considered to be the case when the properties of the bulk gas – gas temperature and relative humidity – are constant at all points in the vicinity of the liquid surface and do not change significantly with the progress of time. This case mostly includes laboratory measurements, where the gas conditions can be kept at a constant value. Or small amount liquid evaporates compared to the large amount of air and this does not significantly modify the gas conditions. Steady-state liquid surface temperature can be established in two ways: if after a sufficiently long period of time the gas and liquid conditions have stabilized; on the other hand, if the surface temperature of the liquid is regulated by heat transfer or heat removal, thus keeping it at a constant value.

2.1. Calculation method

Among the correlations suitable for determining the evaporation rate, the dimensionless, Sherwood equation was chosen. The newly created dimensionless correlation for the Sherwood number also takes into account the driving force of temperature and humidity, which was determined by dimensional analysis (Appendix). Based on this, in addition to the Re number, the new Sherwood equation includes the Sc number and the correction terms that take into account temperatures (ϕ_T), and the value of the partial vapor pressure difference of the gas and the air pressure above the liquid surface (ϕ_P). In addition to the former terms, the Ri number is also included, which enables the combined treatment of evaporation under mixed or forced convection, as this dimensionless quantity is suitable for distinguishing the nature of the gas flow. In this case, the general form of the new dimensionless correlation is as follows:

$$Sh = ARi^B Re^C Sc^D \phi_T^E \phi_P^F. \quad (3)$$

To create the new dimensionless equation, we used measurement results in which the evaporation took place from a container with a free and calm liquid surface under steady-state gas and liquid conditions. We only used measurement results, not simulation data, and the effect of local gas turbulence and liquid convective flow on evaporation was not taken into account. The used datasets included own measurement

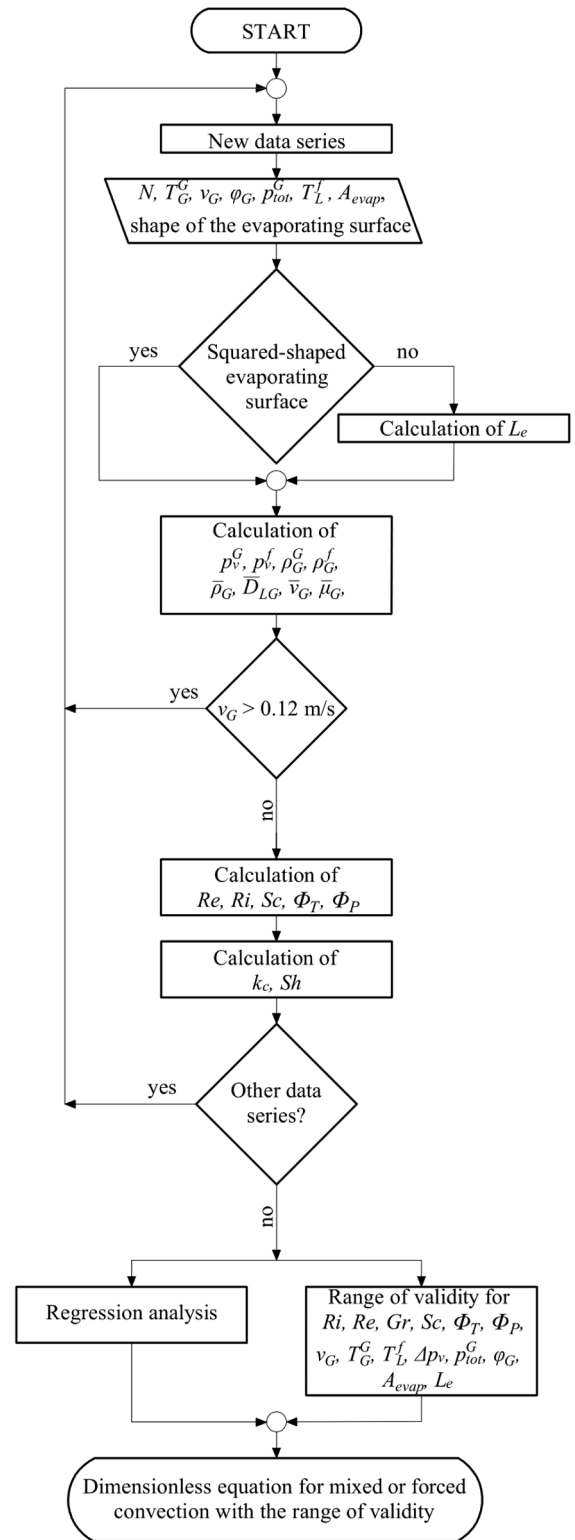


Fig. 1. Flow chart for creating the new dimensionless equation based on measurement data for mixed or forced convection.

results and literature results as well. The flow chart in Fig. 1 shows the steps for processing the measurement results in the case of evaporation under mixed or forced convection.

What hinders the reproducibility and processability of the literature results and thus makes their application uncertain is the inadequate detailing - or even the complete absence, of the ranges of validity and use of the equations. In order to be able to create the Sherwood equation

describing the given evaporation case, knowledge of these measurement conditions is essential. This requires the following data: evaporation rate (N), gas temperature (T_G^G), gas velocity (v_G), gas relative humidity (φ_G), gas pressure above the liquid surface (p_{tot}^G), liquid surface temperature (T_L^f), liquid surface size (A_{evap} , L) and geometry. In some cases, however, the authors did not provide these seven basic parameters in the publication, but other parameters from which they can be calculated.

In the case of markings that use both the subscript and superscript during the calculations, the subscript indicates the medium for which the given parameter should be determined, the superscript indicates the temperature at which the given parameter should be determined. The value of the gas-related characteristics must be determined at the average temperature of the surface of the liquid and of the bulk of the air. The characteristics for air also take into account the humidity content [55]. The saturation vapor pressure of water vapor was determined using the Antoine equation [56], while the diffusion coefficient of air was determined according to McCabe et al. [57].

The dimensionless numbers for evaporation (Sh , Gr , Re , Ri) usually include the characteristic length, which characterizes the evaporating liquid surface in case of evaporation. The sizes and geometries of the liquid reservoirs described in the publications were different, so the equivalent characteristic length (L_e) was introduced in order to make the results comparable. The equivalent characteristic length is equal to the side length of the square whose surface is the same size as the surface of the evaporating liquid:

$$L_e = \sqrt{A_{evap}}. \quad (4)$$

After this, it is necessary to determine the gas and liquid characteristics in order to carry out further calculations. Based on our previous experience in evaporation, we designated $v_G = 0.12$ m/s as the limit value between natural and mixed or forced convection, which was also confirmed by source [8]. Thus, if $v_G > 0.12$ m/s, the data series was used for the case of evaporation with mixed or forced convection. The mixed and forced convection categories were treated together when creating the dimensionless equation, because there were also cases in the literature where the evaporation rate was described with one correlation for several gas convection categories using the Ri number or the air velocity [1,2,10]. Furthermore, the $Sh - Re$ diagram does not show an inflection point or a sharp change in the slope, so there is no obstacle to treating the two gas convection categories together.

The Ri number can be defined as follows:

$$Ri = \frac{Gr}{Re^2}. \quad (5)$$

The Gr number in the Ri number can be calculated with the following relationship:

$$Gr = (\rho_G^G - \rho_G^f) \frac{L_e^3 g \bar{\rho}_G}{\mu_G^2}, \quad (6)$$

while the Re number can be determined with the following equation:

$$Re = \frac{v_G L_e}{\bar{\nu}_G}. \quad (7)$$

The Sc number is a quantity expressing the ratio of the kinematic viscosity and the diffusion factor:

$$Sc = \frac{\bar{\nu}_G}{D_{LG}}. \quad (8)$$

After determining the Sc number, the calculation of the correction terms resulting from the difference in temperature and humidity follows:

$$\Phi_T = \frac{T_G^G + 273.15}{T_L^f + 273.15}, \quad (9)$$

$$\Phi_P = \frac{\Delta p_v}{p_{tot}^G}. \quad (10)$$

In the case of evaporation, unimolar diffusion typically takes place in a two-component system, where the role of the diffusing component is filled by the vapor of the liquid, while the inert component is air. For unimolar diffusion, if the concentration is given by molar concentration, then the molar current density is as follows:

$$N_c = k_c (c_v^f - c_v^G), \quad (11)$$

where k_c is the mass transfer coefficient interpreted in terms of molar concentrations. Molar concentrations can be given using the universal gas law, where the partial pressure of water vapor at the given point, the universal gas constant and the air temperature are used. Since molar current density is used in Eq. (11), while mass current density is used in most publications, the molar mass creates a connection between the two. Thus, the mass transfer coefficient can be determined from the following relationship:

$$N = M_L k_c \left(\frac{p_v^f}{R(T_L^f + 273.15)} - \frac{p_v^G}{R(T_G^G + 273.15)} \right). \quad (12)$$

Finally, the Sh number can be calculated with the help of the mass transfer coefficient which was interpreted in terms of molar concentrations:

$$Sh = \frac{k_c L_e}{D_{LG}}. \quad (13)$$

Using the described calculation method, the coefficient (A) and exponents (B, C, D, E, F) in Eq. (3) can be determined from the measurement results in the literature using regression analysis to describe evaporation under mixed or forced convection. MathWorks MATLAB software was used for the regression analysis. When optimizing the value of parameters A, B, C, D, E, F in the dimensionless equation, the objective function was the minimization of the relative deviations between the Sh numbers calculated from the measurement data (Sh_{meas}) and the Sh numbers calculated from the equation (Sh_{pred}):

$$\delta Sh_{min} = \min \left(\sum_{i=1}^j \frac{|Sh_{pred,i} - Sh_{meas,i}|}{Sh_{pred,i}} \right). \quad (14)$$

During the optimization, we developed a partial factorial design to determine the value of each parameter. First, we examined the results obtained by changing the exponents with a large step interval ($\Delta h = 1$) in a wide interpretation range ($-10 \leq A \dots F \leq 10$). We changed each parameter in the given range according to the step interval, and then we determined the value of the objective function for each possible parameter combination. The range of exponents giving the best results was further narrowed according to the results obtained and according to the values that can often be found in the literature for the given parameter. In addition, it was also important that the parameters were rounded to the appropriate value from an engineering point of view. After the calculation, the program provides the results for the combination of all parameters, from which the combination that gave the smallest Sh_{min} value can be selected. The validity range of the equations, i.e. the limit values of the application for each parameter ($Re, Ri, Sc, \Phi_T, \Phi_P, v_G, T_G^G, T_L^f, \Delta p_v, p_{tot}^G, \varphi_G, Y_G, A_{evap}, L_e$) can be determined from the minimum and maximum values of the data set used. In this way, a new Sherwood equation describing the phenomenon of evaporation more precisely can be created for the given case of evaporation.

2.2. Measuring equipment and measurement method

In addition to the measurement results found in literature publications, we performed measurements for evaporation under mixed or

Table 2
Equipment Specifications and Characteristics.

ID	Designation	Type	Characteristics
IF-1	Conical air inlet	ILKNU-50	$\frac{d_k}{d_b} = \frac{285}{200} mm$ $x = 50 mm$
OP-1	Orifice flow meter	DIRU	$d = 200 mm$, $\Delta p_{max} = 2300 Pa$ $K = 7 - 30$
HV-1	Butterfly valve	Unique production	$d = 200 mm$
RF-1	Cross section change element	Unique production	$\phi 200 mm \rightarrow \square 375 \times 375 mm$
H-101	Electric air heater	Thermo-Team LF-36	$9 + 6 kW_{fix} + 21 kW$ adjustable performance
RF-2	Cross section change element	Unique production	$\square 375 \times 375 mm$ $\square 265 \times 265 mm$
C-101	Radial fan	NVH-50VF/2880-K4-J270	$d = 500 mm$ $n_{max} = 2880 \frac{1}{min}$ $P = 4 kW$, $\dot{V}_{max} = 3240 m^3/h$
FL-1	Flow smoothing element	Unique production	flow distribution insert +Hv 6–7.5–1 perforated steel plate (hexagonal perforation with diagonal division, 63 % free permeable surface)
FD-1	Flow deflector element	Unique production	5 curved plates 130 mm wide
FL-2	Flow smoothing element	Unique production	flow distribution insert +Hv 6–7.5–1 perforated steel plate (hexagonal perforation with diagonal division, 63 % free permeable surface)
RF-3	Cross section change element	Unique production	$245 \times 130 mm$ $300 \times 350 mm$
FL-3	Flow smoothing element	Unique production	1670 red copper pipes $\phi 8 \times 1 - 100 mm$
E-101	Evaporation section	Unique production	$300 \times 350 - 1000 mm$
V-101	Evaporation tray	Stainless steal	size $220 \times 290 \times 8 mm$ $A_{evap} = 0.0627 m^2$ $V = 0.55 l$
EL-1	Manual lift	Unique production	$340 \times 400 mm$ $\Delta z = 150 mm$
RF-4	Cross section change element	Unique production	$300 \times 350 mm \rightarrow \phi 200 mm$

forced convection using the measuring station located at the Department. The image of the measuring device can be seen in Fig. 2, the piping and instrumentation diagram with instrument elements and air duct line elements is presented in Fig. 3. The parts of the measuring equipment and their characteristics are described in Table 2.

The air is circulated by an NVH-50VF/2880-K4-J270 type radial fan (C-101) driven by a 4 kW electric motor ($n_{max} = 2880 \text{ 1/min}$). The suction section starts with a 200 mm diameter INKLU-50 cone-shaped inlet (IF-1) equipped with a mesh filter. The inlet is followed by the Lindab DIRU-200 orifice flow meter (OP-1), which has a variable throat diameter due to its iris design. There is a free flow length of 6D in front of the orifice flow meter and 4D after it, thus ensuring the undisturbed air flow required for volume flow measurement. Coarse adjustment of the air velocity is possible by turning the butterfly valve built into the air duct (HV-1), and fine adjustment is possible by changing the fan speed with a frequency converter. To increase the air temperature, a ThermoTeam LF-36 type electric heater (H-101) is available, which consists of 9 +6 kW fixed and 21 kW $\pm 0.5^\circ\text{C}$ adjustable heating inserts. In the air duct, after the fan, honeycomb plates, flow distribution inserts (FL-1, FL-2), flow diverting plates (FD-1) and red copper flow smoothing tubes (FL-3) – piece of 1670, with an outer diameter of 8 mm, a wall thickness of 1 mm, and a length of 100 mm – are arranged for a uniform, laminar flow of air.

In the tested air duct section (E-101), the liquid evaporates from an 8 mm thick tray (V-101), which is placed in 40 mm thick XPS thermal insulation plates. The amount of liquid that can be filled into the tray is

Table 3
Instrumentation Specification.

ID	Designation	Measured quantity	Range and accuracy
TR-101	ALMEMO D6 FHAD 36 Rx digital temperature and humidity meter	Ambient temperature of dry air	$-100 - 200^\circ\text{C}$ $\pm 0.2^\circ\text{C}$
PR-101	ALMEMO D6 FHAD 36 Rx digital temperature and humidity meter	Pressure of ambient air	700 – 1100 mbar $\pm 2.5 \text{ mbar}$
XR-101	ALMEMO D6 FHAD 36 Rx digital temperature and humidity meter	Relative humidity of ambient air	0 – 100 % $\pm 1.3 \%$
PDI-101	MTA Kutesz U-tube manometer	Pressure difference measured on the orifice flow meter	0 – 400 Pa $\pm 10 \text{ Pa}$
PDR-101	Pressure transmitter; Ahlborn	Pressure difference measured on the orifice flow meter	0 – 4000 Pa $\pm 10 \text{ Pa}$
TIC-101	JUMO ITRON 04 air heating temperature controller	Air flow temperature regulator	$T_{amb} - 100^\circ\text{C}$ $\pm 0.5^\circ\text{C}$
TT-101	PT100 temperature transmitter	Air flow temperature	$-500 - 250^\circ\text{C}$ $\pm 0.1^\circ\text{C}$
SIC-101	Schneider Electric Altivar 312 frequency converter	Regulate air after the heater	0 – 2880 1/min
TR-102	ALMEMO D6 FHAD 36 Rx digital temperature and humidity meter	Ambient temperature of dry air	$-100 - 200^\circ\text{C}$ $\pm 0.2^\circ\text{C}$
PR-102	ALMEMO D6 FHAD 36 Rx digital temperature and humidity meter	Pressure of ambient air	700 – 1100 mbar $\pm 2.5 \text{ mbar}$
XR-102	ALMEMO D6 FHAD 36 Rx digital temperature and humidity meter	Relative humidity of ambient air	0 – 100 % $\pm 1.3 \%$
TR-103	T-type thermocouple	Bulk temperature of liquid	$-200 - 400^\circ\text{C}$ $\pm 0.1^\circ\text{C}$
TR-104	AHLBORN AMiR 7842 infrared meter	Liquid surface temperature	0 – 500 $^\circ\text{C}$ $\pm 1^\circ\text{C}$
WIR-101	Sartorius Signum 1 scale	Mass of evaporated liquid	0 – 65 kg $\pm 1 \text{ g}$
HV-101	Manually regulated butterfly valve	Air flow velocity	
ES-101	Air heater electric switch	Switching on the heating of air flow	

0.55 liters, its evaporating surface open to the environment is 0.0627m^2 , its characteristic length in the direction of flow is $L = 220 \text{ mm}$. The heat-insulated tray is located on a manually adjustable scissor lift (EL-1), with which the liquid level can be adjusted to the lower plane of the air duct. After the evaporation measurement section, the moist air is released into the environment through an outlet pipe. The air duct of the measuring equipment, from the electric air heater to the end of the evaporation measuring section, is insulated with 20 mm perforated rock wool.

During the measurement, an Ahlborn D6 FHAD 36 Rx hygrometer measures the dry temperature (TR-101, TR-102), air pressure (PR-101, PR-102) and relative humidity (XR-101, XR – 102) of the ambient air and the air in the evaporation section. The pressure difference occurring on the orifice flow meter is measured by a U-tube manometer (PDI-101) and an Ahlborn DPS (PDR-101) pressure transmitter installed in parallel with it. A Sartorius Signum 1 type (WIR-101) digital scale is used to measure the mass of the tray and the liquid together. An AMiR 7842 type infrared thermometer (TR-104) placed 80 mm above the liquid level is used to measure the surface temperature of the liquid, and a T-type thermocouple is used to measure the bulk temperature of the liquid (TR-103). Each sensor is connected to an Ahlborn ALMEMO 2890-9 type data logger to record evaporation characteristics. The measured values are recorded by the Apollo module of the IMPERIUM Laboratory Information System [58], on which the sampling recording frequency can be set.

The measurement starts by filling the tray (V-101) with liquid. After starting the fan (C-101), the air velocity can be adjusted by using the butterfly valve (HV-101) and the frequency converter (SIC-101), which can be checked using the pressure difference (PDR-101) measured on the orifice flow meter. By switching on (ES-101) the electric air heater (H-101), the required air temperature (TR-102) can be created. Before starting the evaporation rate measurement, the equipment must be run empty until the stationary state is reached (until the values measured by the thermometers are stabilized). Before starting the measurement, it is necessary to replace the amount of liquid that has evaporated until then. Then, in addition to recording the data measured by the instruments, the measurement for liquid evaporation takes approx. 2 h. The types and characteristics of the measuring devices and regulators placed on the measuring equipment are described in Table 3.

2.3. Statistical method

The created new dimensionless equation was compared with the literature correlations for the given evaporation case by substituting the used measurement data series. The value of the evaporation rate (N) was determined for a given set of measurement data with the analyzed correlation. Knowing the value of the evaporation rate, based on Eq. (12), the mass transfer coefficient (k_c) can be expressed and calculated. Substituting the mass transfer coefficient into the Eq. (13), the Sh_{pred} number can be calculated. This calculation had to be performed for all measurement data sets. Then, by substituting the Sh_{pred} numbers and the Sh_{pred} numbers calculated from the measurement results into the Eqs. (15)–(18), various statistical indicators (MAE; RE; RMSE; R^2) can be determined. These statistical indicators can be defined for the examination of the new dimensionless equation and the correlations in the literature, which can be used to select the equation that best approximates the measurement results [59,60].

When calculating the mean absolute error (MAE, [1]), we take the average of the deviations between the calculated and measured values, which is equal to 0 in the case of a good fit. The disadvantage of its application is that the direction of deviation is not taken into account:

$$MAE = \frac{1}{j} \sum_{i=1}^j |Sh_{pred,i} - Sh_{meas,i}|. \quad (15)$$

The average relative error (RE, [1]) shows the average of the ratio of the absolute error to the measured value, approaching 0 in the case of a good fit:

Table 4

Limit values of statistical indicators.

\bar{w}	MAE	RE	RMSE	R^2
Max. (100 points)	0	0	0	1
Min. (0 points)	MAE_{max}	RE_{max}	$RMSE_{max}$	R^2_{min}

$$RE = \frac{1}{j} \sum_{i=1}^j \frac{|Sh_{pred,i} - Sh_{meas,i}|}{Sh_{pred,i}} \quad (16)$$

The root mean square error ($RMSE$, [1]) shows how much the data is scattered around the regression line. The smaller its value, the better the relationship between the calculated and measured value. The disadvantage of its use is that it is sensitive to large deviations:

$$RMSE = \sqrt{\frac{1}{j} \sum_{i=1}^j (Sh_{pred,i} - Sh_{meas,i})^2} \quad (17)$$

The coefficient of determination (R^2 , [1]) can be used to characterize the fit between calculated and measured values. The better the fit, the closer its value is to 1, but it is sensitive to outliers:

$$R^2 = 1 - \frac{\sum_{i=1}^{i=j} (Sh_{pred,i} - Sh_{meas,i})^2}{\sum_{i=1}^{i=j} (Sh_{meas,i} - \bar{Sh}_{meas})^2} \quad (18)$$

During the comparison, the values of the four types of statistical indicators were determined for all the equations belonging to the given case. In order to be able to choose the best correlation for the calculation of the evaporation rate, the equations were organized according to the statistical indicators. Those correlations that, according to one of the statistical indicators, gave a bad value as an outlier, were not taken into account during the systematization. Such an outlier was when $RE > 1$ or $R^2 < 0$. The reason for this was that, in the case of the scoring system, the examined statistical indicators would have covered a large range, in which the equations giving better results would have appeared only in a narrow interval. This would have reduced the difference between the scores of the better performing equations.

In order to be able to take into account the results given by all four statistical indicators and to select the best correlation for the calculation of the evaporation rate based on them, the equations can be organized according to the individual statistical indicators. For this, each equation receives a score between 0 and 100 points for a given statistical indicator. The highest score is given to the equation when it achieves the best result according to the given indicator, that is, when the calculated value exactly matches the measured value. These values can be seen in the 'maximum (100 points)' row of Table 4. The values in the 'minimum (0 points)' line of the table indicate the maximum value of the statistical indicators. The minimum value is the largest value among the statistical indicators determined for the tested equations. In this way, a range can be created where the maximum score can only be given to the equation if the result is exactly the same, while the minimum score is given to the

equation that achieves the worst result.

This type of systematization is suitable because it also takes into account the magnitude of the differences between the results given by the equations. However, this can also be a disadvantage, because if the data series contains an outlier, the difference between the minimum and maximum value increases. Although the order of the equations remains the same, the scores obtained change proportionally. Because of the latter problem, the equations involved in the scoring system must be filtered in advance, so the scores that better represent the real results can be obtained.

If the range covered by the given statistical indicator is available, the obtained score can be determined by linear interpolation according to the agreement between the measured and calculated values. This calculation must be performed for each indicator for the results given by all the equations. In the case of a given correlation, the score obtained by four types of statistical indicators was averaged to establish the final order:

$$\omega_{tot} = \frac{\bar{w}_{MAE} + \bar{w}_{RE} + \bar{w}_{RMSE} + \bar{w}_{R^2}}{4} \quad (19)$$

According to the final score, the equations can be ranked, and the correlation with the highest score can be used with the highest accuracy to determine the value of the evaporation rate.

3. Results and discussion

During our research, we used the publications that provided a sufficient amount of information to determine Sherwood equation. Among the cases of evaporation [54], we examined evaporation with the steady-state gas and liquid conditions. Thus, our goal was to create a new Sherwood equation describing the evaporation rate for the case of evaporation with steady-state gas and liquid conditions, based on which even other evaporation cases can be investigated.

3.1. Measurement results

Table 5 contains the publications examined under mixed or forced convection, which were used in the creation of the new dimensionless equation. Only a few publications in the literature contained measurement results for water evaporation that could have been used. The reason for this is mainly the absence of the values of the seven basic parameters, without the calculation according to the algorithm shown in Fig. 1 cannot be performed. In most cases, the value of the air pressure above the liquid surface was not reported in the publications. In order to still be able to use the literature results, an approximate value was determined based on the location of the measurement, the height above sea level and the specified temperature [61]. In the case of the measurements presented in these publications, the typical size of the tank containing the liquid was small ($L_e < 1.5$ m), and thus evaporation can be considered with steady-state gas and liquid conditions.

In addition to the above publications, other research results can be found in the literature, where the measurement results were described with appropriate parameters, but they did not belong to the case with steady-state gas and liquid conditions [65–68] or they did not describe the evaporation of water [15,26]. Thus, these measurement results were not taken into account when creating the equation. Rohwer's publication [23] belongs to the evaporation case with a varying gas conditions, but we still used his measurement results to describe the case with a steady-state gas conditions. This was possible because he provided differentiated data for each sampling time in his measurements. The second column of the table shows the number of measurement data series found in each publication. In some cases [10,23,44], there were outliers in the data series that could clearly be considered measurement errors, so they were removed from the data series. The number of the original data series is in the parenthesis, while in front of it is the quantity of the measurement data series that was used during the

Table 5

Publications and measurement results used for the new dimensionless equation for evaporation under mixed or forced convection.

Publications	Number of measurements
Blazquez et al. [62]	26 (27)
Asdrubali [63]	33
Yen and Landvatter [44]	59 (60)
Pauken [10]	36 (47)
Raimundo et al. [52]	24
Inan and Atayilmaz [53]	9
Gallero et al. [64]	32
Varju and Poós	32
Rohwer [23]	268 (278)

Notation: The second column contains the number of the data series used, while the number in the parentheses is the full data series.

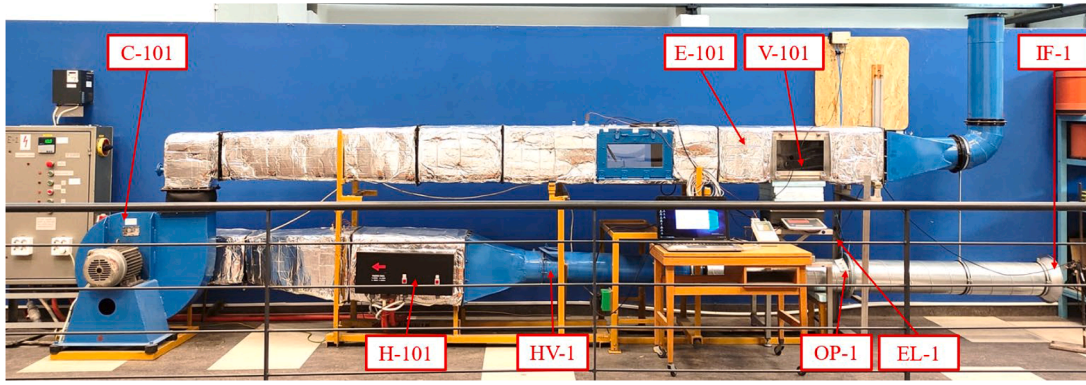


Fig. 2. Measuring equipment for evaporation rate determination.

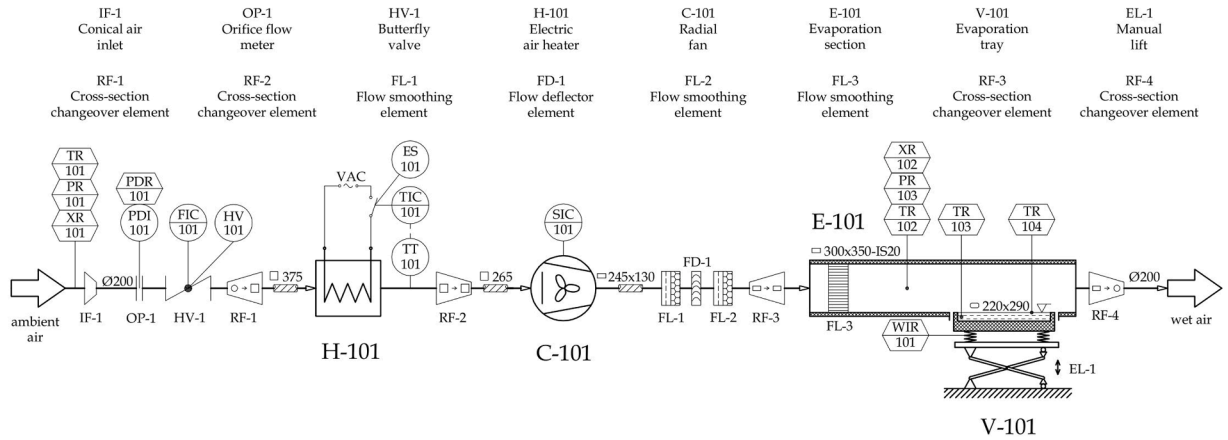


Fig. 3. Technological process diagram of the measuring equipment suitable for testing evaporation rates with instrument elements and main air duct line elements. Statistical method.

evaluation.

On the laboratory measuring equipment, we investigated the case of evaporation for water at steady-state gas and liquid conditions, at different air velocities and air temperatures. Thus, we performed a total of 32 measurements for water evaporation, Table 6 contains the results. The measurement results shown in the table are arranged according to air temperature and air velocity.

3.2. Determination of dimensionless equation

For the case of evaporation with steady-state gas and liquid conditions under mixed or forced convection, the existence of the basic parameters was fulfilled in a total of 8 publications in the literature. Thus, 519 measurement data series were available, all of which examined water evaporation. The calculation algorithm shown in Fig. 1 can be used to determine the necessary parameters for the new dimensionless equation. During the calculation of the Ri number, the absolute value of the Gr number was taken, ignoring the flow direction caused by the density difference.

Based on the available data, the dimensionless numbers included in the new dimensionless equation $Sh, Ri, Re, Sc, \Phi_T, \Phi_p$ were determined. The values of coefficients $A \dots F$ and exponents in Eq. (3) can be determined according to the method described in Chapter 2.1. During the optimization, the tested ranges of the parameters were chosen based on literature recommendations and preliminary optimum searches. Thus, after running the calculation, we selected from among the results the parameter combination for which the value obtained by Eq. (14) was the smallest. Due to the applied conditions, the obtained parameter values are also acceptable from an engineering point of view with

decimal digits, thanks to which we obtained a more relevant equation.

The final form of the dimensionless equation for evaporation cases with steady-state gas and liquid conditions under mixed or forced convection:

$$Sh = 0.24 Ri^{0.03} Re^{0.7} Sc^{1/3} \Phi_T^{-2} \Phi_p^{0.1}, \quad (20)$$

in the following validity range and measurement conditions:

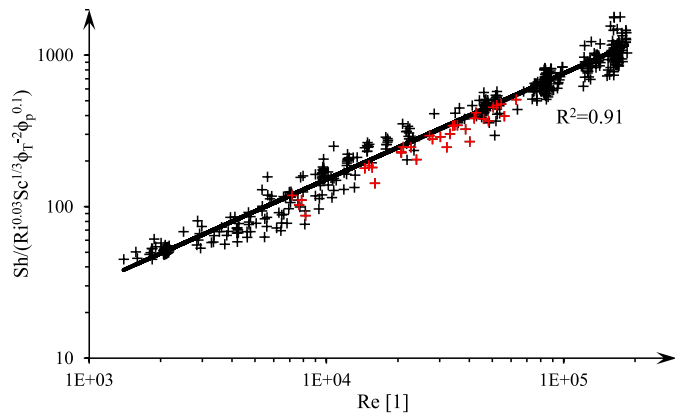
$$\begin{aligned} 2.34 \cdot 10^{-6} &\leq Ri < 7.4 & -19^\circ C &\leq T_G^C \leq 79^\circ C \\ 1400 &\leq Re \leq 1.85 \cdot 10^5 & 0.17 \text{ m/s} &\leq v_G \leq 5.7 \text{ m/s} \\ 3.27 \cdot 10^4 &\leq Gr \leq 8.47 \cdot 10^9 & 4\% &\leq \varphi_G \leq 99\% \\ 0.58 &\leq Sc \leq 0.7 & 0.5 \text{ g/kg} &\leq Y_G \leq 47 \text{ g/kg} \\ 0.88 &\leq \Phi_T \leq 1.15 & 25 \text{ Pa} &\leq \Delta p_v \leq 10,000 \text{ Pa} \\ 0.0003 &\leq \Phi_p \leq 0.1 & 84,300 \text{ Pa} &\leq p_{tot}^G \leq 101,400 \text{ Pa} \\ & & 1^\circ C &\leq T_L^C \leq 61^\circ C \\ & & 0.015 \text{ m}^2 &\leq A_{evap} \leq 1.09 \text{ m}^2 \\ & & 0.12 \text{ m} &\leq L_e \leq 1.04 \text{ m} \end{aligned}$$

Validity ranges give the limits of the intervals covered by the analysed data series. The average relative error of the equation is 12.4 %. Fig. 4 shows the $Sh - Re$ function relationship, where the data points marked in black are from the literature, while the data points marked in red are the results of our own measurements. It can be seen that the own measurement results complement well the results of the literature measurements, that is, the structure of the measuring equipment and the measurement method were appropriate. It can be concluded that when the measurement data series are plotted on a logarithmic scale, the points are arranged around a straight line.

Table 6

Results of evaporation measurements on the own measuring equipment.

No.	v_G $\frac{m}{s}$	T_G^o $^{\circ}C$	φ_G %	p_{tot}^G Pa	T_L^f $^{\circ}C$	N $\frac{kg}{(m^2h)}$
1	0.51	30.1	34.5	100,675	22.4	0.136
2	1.00	29.7	27.8	100,572	21.9	0.252
3	1.48	30.5	25.9	101,445	19.3	0.262
4	2.00	30.6	25.8	101,339	20.5	0.364
5	2.49	29.8	24.8	99,594	20.2	0.410
6	2.98	30.1	25.3	100,710	18.5	0.429
7	3.47	30.1	19.9	101,164	17.7	0.512
8	3.93	32.9	19.3	100,723	18.6	0.664
9	0.49	40.4	19.2	100,283	24.2	0.212
10	1.00	40.5	15.9	100,469	22.4	0.338
11	1.46	40.6	18.6	100,639	23.0	0.418
12	1.93	39.4	13.9	100,691	20.9	0.501
13	2.49	40.6	19.2	100,593	23.1	0.523
14	2.99	41.5	24.9	99,615	25.4	0.578
15	3.51	40.2	19.3	100,005	23.6	0.815
16	0.52	50.2	8.9	100,992	24.5	0.285
17	1.00	50.3	9.4	100,884	24.7	0.456
18	1.37	49.0	13.2	100,368	25.3	0.482
19	1.82	50.4	16.2	100,151	27.6	0.620
20	2.31	49.5	14.1	100,342	26.3	0.732
21	2.80	50.1	14.0	99,934	26.6	0.810
22	3.49	50.5	14.5	100,021	26.4	0.903
23	0.49	60.2	5.5	101,049	26.7	0.378
24	1.00	59.4	6.0	100,827	27.1	0.558
25	1.46	60.0	8.9	100,085	28.5	0.675
26	1.93	59.3	10.4	100,033	29.0	0.717
27	2.46	59.7	10.2	99,729	29.6	0.927
28	2.95	60.6	8.7	100,303	28.5	1.083
29	3.50	62.2	6.5	100,078	28.1	1.289
30	1.47	69.3	5.4	100,140	29.9	0.761
31	2.44	70.5	6.7	99,901	31.5	1.098
32	2.43	79.1	3.7	99,981	32.1	1.192

**Fig. 4.** The new dimensionless equation created for the case of evaporation with steady-state gas and liquid conditions under mixed or forced convection and the measurement results (own measurements are marked in red).

3.3. Comparison of the equations

The new dimensionless equation valid for evaporation under mixed or forced convection was compared with the correlations from

Table 1, which belonged to the evaporation case with steady-state gas and liquid conditions. To do this, we compared the Sh numbers obtained from literature correlations with the Sh numbers calculated from the measurement data series using the statistical indicators and classification method found in Chapter 2.3. If the validity range of the given equation was not available, the calculation was performed for the entire measurement data series. If the validity range of the equations was known, or partially known, we still performed the calculations for

Table 7

The values of the statistical indicators calculated for the new dimensionless equation under mixed or forced convection and the literature correlations.

Ref.	Equation	MAE [1]	RE [%]	RMSE [1]	R ² [1]
[20]	Varju and Poós	25.6	12.4	43.1	0.91
[13]	Himus and Hinchley	73.2	29.1	94.1	0.59
[18]	Thiesenhusen	81.1	25.3	106.9	0.47
[28]	Lurie and Michailoff	65.2	24.4	86.7	0.65
[14]	Leven	48.5	17.4	70.7	0.77
[22]	Smolsky and Sergeyev	52.4	36.4	74.7	0.71
[44]/a	Yen and Landvatter	58.6	48.3	81.0	0.69
[44]/b	Yen and Landvatter	226.8	38.0	374.7	−5.55
[45]	Baturin	45.9	44.2	61.5	0.82
[46]	Bennett and Meyers	87.9	57.9	122.8	0.30
[48]	Sartori	121.0	142.8	150.6	−0.06
[15]/a,b	Braun and Caplan	63.1	44.2	80.5	0.70
[15]/c,d	Braun and Caplan	154.4	40.1	196.6	−0.80
[49]	Rotkegel	79.0	95.1	103.3	0.50
[39]	Hummel et al.	47.0	25.2	71.1	0.76
[10]/a	Pauken	61.5	20.4	98.8	0.64
[10]/b	Pauken	65.0	26.3	100.7	0.53
[30]/a,b	Al-Shammiri	187.9	264.7	295.0	−3.06
[11]/b	Moghiman and Jodat	40.1	17.5	60.1	0.83
[2]/a	Jodat et al.	116.5	32.0	205.5	−0.97
[2]/b	Jodat et al.	194.6	40.2	266.2	−2.31
[51]	Yanagi et al.	71.4	21.4	100.3	0.53
[26]	Heymes et al.	42.6	29.3	67.6	0.79
[52]/a	Raimundo et al.	40.0	18.0	56.8	0.85
[52]/b	Raimundo et al.	111.2	61.0	159.6	−0.19
[53]	Inan and Atayilmaz	143.4	49.0	214.0	−1.14

Table 8

The limit values of the statistical indicators for correlations suitable for determining the evaporation rate under mixed or forced convection.

\bar{w}	MAE	RE	RMSE	R ²
Max. (100 points)	0	0	0	1
Min. (0 points)	87.9	95.1	122.8	0.3

Table 9

Scoring results of the comparison of the new dimensionless equation and literature correlations for evaporation under mixed or forced convection.

Nr.	Ref.	Equation	\bar{w}_{MAE} [1]	\bar{w}_{RE} [1]	\bar{w}_{RMSE} [1]	\bar{w}_{R^2} [1]	w_{tot} [1]
1	[20]	Varju and Poós	70.9	87.0	64.9	87.7	77.6
2	[52]/a	Raimundo et al.	54.4	81.1	53.7	78.6	67.0
3	[11]/b	Moghiman and Jodat	54.4	81.6	51.0	76.0	65.8
4	[14]	Leven	44.8	81.7	42.4	66.9	59.0
5	[26]	Heymes et al.	51.6	69.2	45.0	69.7	58.9
6	[39]	Hummel et al.	46.6	73.5	42.1	66.4	57.1
7	[45]	Baturin	47.8	53.5	49.9	74.9	56.6
8	[22]	Smolsky and Sergeyev	40.3	61.7	39.2	58.8	50.0
9	[28]	Lurie and Michailoff	25.8	74.3	29.4	50.1	44.9
10	[10]/b	Pauken	30.0	78.5	19.5	49.1	44.3
11	[15]/a, b	Braun and Caplan	28.2	53.5	34.4	57.0	43.3
12	[44]/a	Yen and Landvatter	33.4	49.2	34.0	56.5	43.3
13	[13]	Himus and Hinchley	16.7	69.4	23.4	41.3	37.7
14	[10]/a	Pauken	26.0	72.3	18.0	32.7	37.2
15	[51]	Yanagi et al.	18.8	77.5	18.3	33.3	37.0
16	[18]	Thiesenhusen	7.7	73.4	12.9	24.2	29.6
17	[49]	Rotkegel	10.1	0.0	15.8	29.2	13.8
18	[46]	Bennett and Meyers	0.0	39.1	0.0	0.0	9.8

the entire measurement data series, as we checked whether their validity range could be extended. The equation of Haji and Chow [36] was not used in the comparison, because it can only be used in the case of flow in a channel, where the air mass flow rate is known. In the measurement data series, the air did not always flow in a channel, or the cross section

of the channel was unknown. The correlation of Chuck and Sparrow [47] also requires the value of the drop in height during liquid loss, which is not known in advance in reality, so we did not use this correlation during the evaluation either. In the equation of Moghiman and Jodat [11]/a, the exponent of the partial vapor pressure difference is given by a third degree polynomial function depending on the air velocity. For this reason, the exponent can even take on a negative or very small value, which results in a bad or incomprehensible value for the evaporation rate, which is why we did not use the equation during the evaluation.

The values of the statistical indicators determined for the Eq. (20) new dimensionless equation and the literature correlations belonging to the same evaporation case can be seen in Table 7. In general, it can be said that the R^2 was high in the case of correlations with a lower RE . The $RMSE$ of the correlations gave the same results as the MAE .

Many of the correlations used resulted in a negative R^2 , an RE greater than 100 %, or high MAE and $RMSE$ [2]/a,b, [15]/c,d, [44]/b, [30, 48]/a,b, [52]/b, [53]; thus, using them would cause a value loaded with a large error during classification. In order to perform the classification on the relevant evaporation rate correlations, we did not consider these equations that gave worse results. So, the ranges of the statistical indicators required for classification were determined only for the best 18 correlations. These ranges are shown in Table 8.

Knowing the ranges, the scores can be calculated for each equation by linear interpolation, and then the final score can be determined by averaging. The scores for the correlations according to the statistical indicators, as well as the final scores, can be found in Table 9.

The correlations of Bennett and Meyers [46] and Rotkegel [49] gave the worst error values, so their extreme values were used for scoring, and therefore their equations received the lowest score. Bennett and Meyers [46] derived their relationship at a theoretical level, so the exponent of the Re number became 0.5, and the Sc number's became 1. The correlation of Bennett and Meyers [46] and Rotkegel [49] also underestimates the evaporation rate over the entire range. Thiesenhusen's equation [18] gave the evaporation rate well for low Sh numbers, while it overestimated the intensity of evaporation for higher Sh numbers. These equations received a total score below 30 points in the classification.

In addition to the air velocity and the partial vapor pressures, Yanagi's equation [51] includes the total pressure and the average density of the air in such a way that it reproduces the evaporation rate well for small Sh numbers, but significantly overestimates it for higher Sh numbers. As Jodat et al. [2], Pauken [10] also created two correlations for the evaporation rate, of which the Eq. [10]/b directly specifies the evaporation rate, gave a worse result. This equation contains the air velocity in the form of a quadratic polynomial, which overestimates the evaporation rate for higher Sh numbers. The equation of Himus and Hinchley [13], on the other hand, slightly overestimates the evaporation rate over the entire range, and in the equation the exponent of the partial vapor pressure difference is still $n = 1$. These equations were graded between 30 and 40 points.

Interestingly, the relation of Braun and Caplan, which is valid for the evaporation of different liquids [15]/a,b describes the evaporation of water better than their relation, which was created only for the evaporation of water [15]/c,d. The former relation of Braun and Caplan [15]/a,b and the modified Sherwood equation of Yen and Landvatter [44]/a underestimates slightly the evaporation rate. Pauken's Sherwood equation [10]/b gave better results than the correlation of Jodat et al. [2]/b. Pauken gave the relationship between the two Sh numbers according to the Ri number only with a quadratic polynomial, which turned out to be better than the cubic one. Lurie and Michailoff's equation [28] slightly overestimates the evaporation rate and in their equation the exponent of the partial vapor pressure difference is still $n = 1$. The equations described so far achieved scores between 40 and 50 points during the classification.

The disadvantage of the equation of Smolsky and Sergeyev [22] is

that if the correction term, the Gu number - which can be calculated from the gas and liquid surface temperatures -, takes a negative value, then the equation cannot be interpreted. We did not take the measurements where this happened into account when determining the statistical indicators. The R^2 of their equation is among the better values, but their results are excessively scattered compared to the Sh number values determined from the measurement. The correlation of Baturin [45] despite taking the exponent of the partial vapor pressure as 1, gave fairly good results, only slightly underestimating the intensity of evaporation. Hummel et al. [39] and Heymes et al. [26] created their correlation by examining not only the evaporation of water, but also that of other volatile liquids. Hummel et al. [39] indicated air velocity, liquid temperature, air pressure, characteristic length and the molar mass of the gas and liquid, among the parameters affecting evaporation, in an attempt to create a more general expression. Heymes et al. [26] described the evaporation rate with a relation giving the Sh number, which included the Re number and the Sc number. Both equations slightly underestimate the intensity of evaporation. In the correlation of Leven [14]/b the exponent of the partial vapor pressure is given as a function of the air velocity, but as a simple ratio, not a polynomial function. The equation gave a better RE value, but its R^2 is lower, and it overestimates the evaporation rate at higher Sh numbers. The presented correlations received a score between 50 and 60 points, so they were placed in the first half of the established order.

The best three correlations (Eq. (20), [52]/a, [1]/b) received a final score of over 60 points. Moghiman and Jodat's equation [11]/b gave a better RE than the correlation of Raimundo et al. [52]/a, but MAE , $RMSE$ and R^2 indicators were better for the latter. Both correlations slightly overestimate the evaporation rate. Furthermore, even though the exponent of the partial pressure difference of water vapor is 1, the correlation of Raimundo et al. [52]/a gave good results for the evaporation. Moghiman and Jodat's equation [11]/b contains the theoretical relations regarding mass transfer under natural and forced convection, with the help of which a combined Sh number was created. The best results were given by the new Eq. (20) dimensionless equation where the RE between the measured and calculated Sh numbers was 12.4 %. Furthermore, the R^2 of the Eq. (20) was the highest value with 0.91, while the $RMSE$ and MAE values were also the best.

For the top three equation (Eq. (20), [52]/a, [1]/b) the calculated Sh_{pred} numbers from the equations are plotted as a function of the Sh_{meas} number determined from the measurement data in the Fig. 5. A similar trend can be observed for all three equations, that the evaporation rate is slightly overestimated. The equation of Moghiman and Jodat [11]/b overestimates the measured values to a greater extent for higher Sh numbers. The equation of Raimundo et al. [52]/a and the new Eq. (20) have the same trend because it follows the 45° straight line, but in the case of the former, the points are more scattered around it.

The Bland-Altman method was used to further investigate the relationship between the Sh number values determined by the three correlations and calculated from the measurement data series [69]. Fig. 6 shows the graphic illustration of the Bland-Altman method in the case of the Sh number calculated from the three empirical correlations and the measurement data series. The agreement was also characterized by specifying the 90 % confidence interval limits, where most of the points should fall within this interval. The results of the Bland-Altman method for the empirical correlations are shown in Table 10. Ideally, the points lie on the abscissa. The difference between the average of the calculated and measured Sh numbers in the case of the new Eq. (20) was exceptionally good, as the value of the axis section was 2. The correlation of Raimundo et al. [52]/a and Moghiman and Jodat [11]/b gave the same order of magnitude, in the case of the former it was 24.8, while in the case of the latter it was 28.7. For both equations, the slope of the line given by the points indicates a proportional error. The confidence interval was the narrowest for the new Eq. (20), which was followed by the equation of Raimundo et al. [52]/a and Moghiman and Jodat [11]/b. The

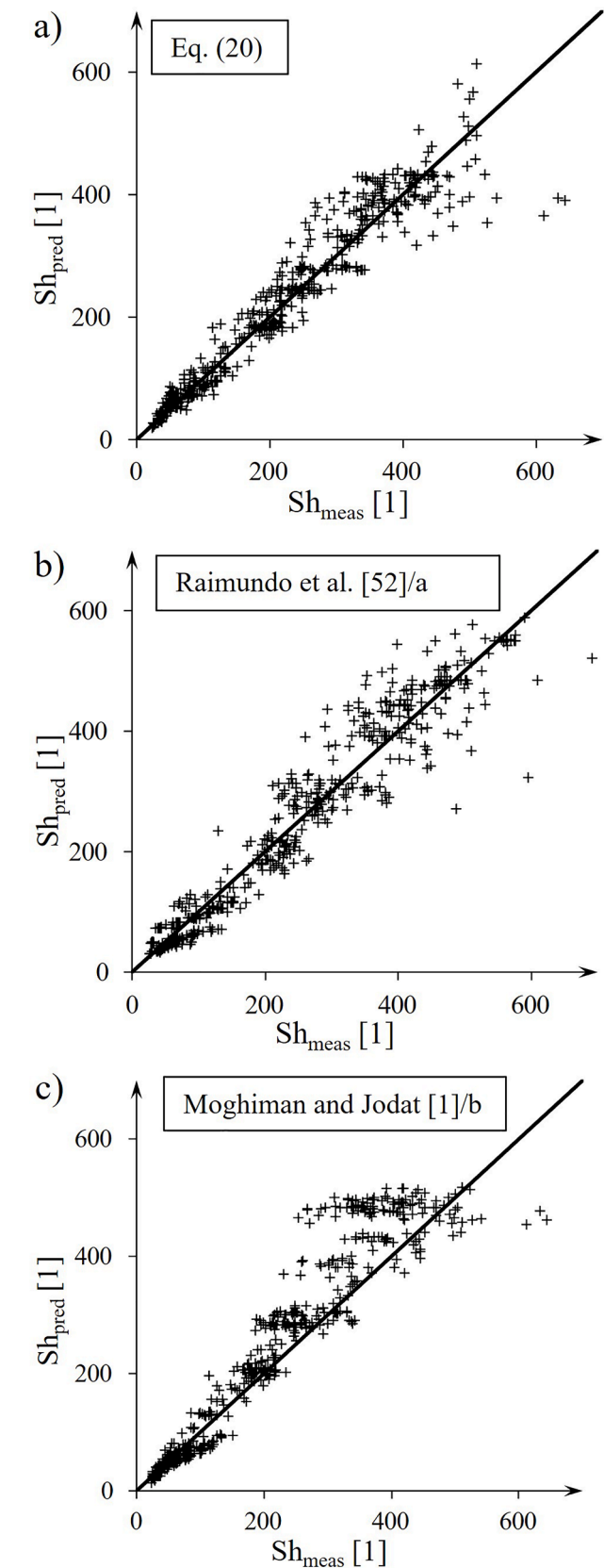


Fig. 5. The calculated and measured Sh number for the best three correlations for evaporation under mixed or forced convection.

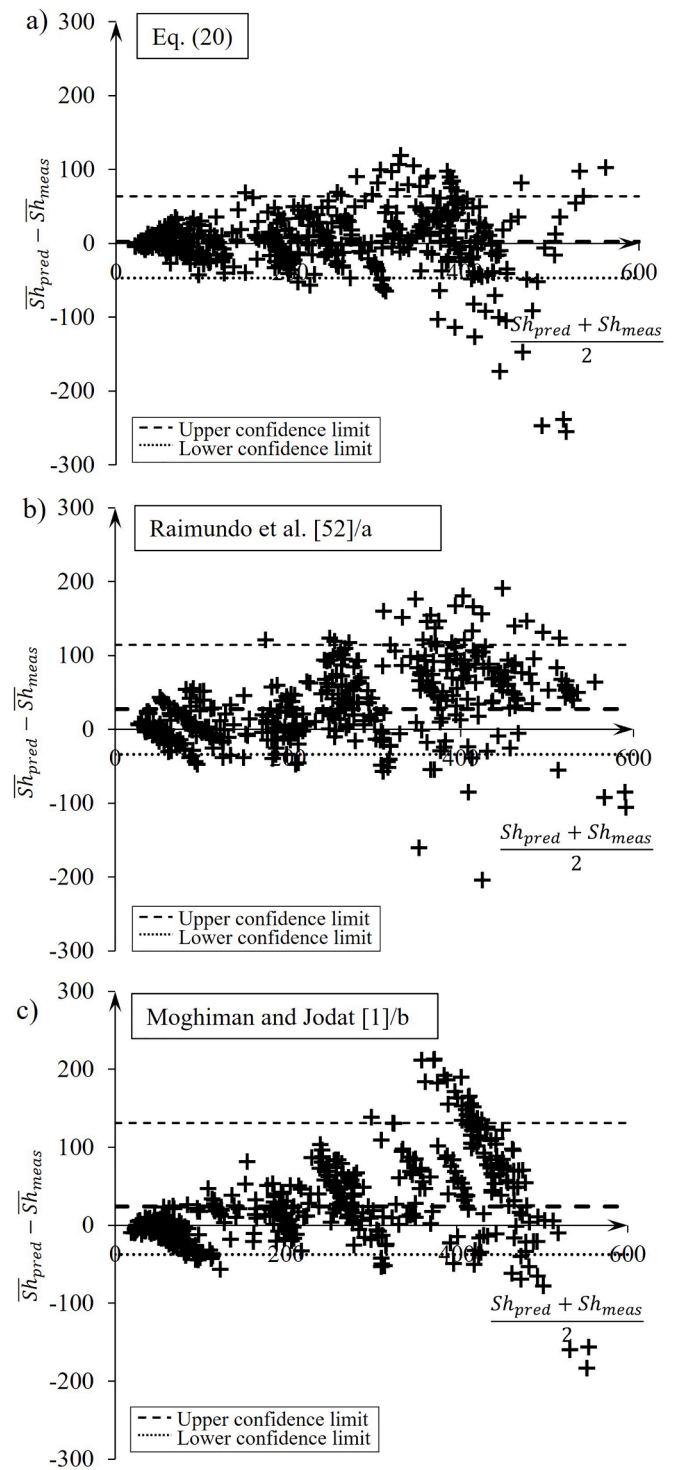


Fig. 6. Examination of the calculated and measured Sh number using the Bland-Altman method for evaporation under mixed or forced convection.

Table 10			
Results of the Bland-Altman method for empirical correlations for evaporation under mixed or forced convection.			
Ref.	Equation	Confidence interval	$\overline{Sh_{pred} - Sh_{meas}}$
[20]	Varju and Poós	110.7	2.0
[52]/a	Raimundo et al.	148.7	24.8
[1]/b	Moghiman and Jodat	168.5	28.7

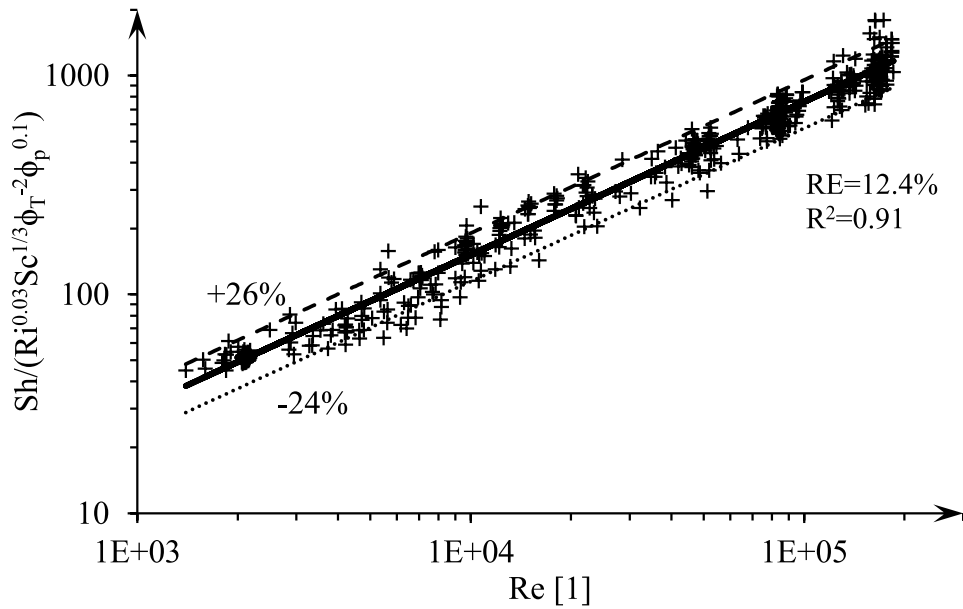


Fig. 7. New dimensionless Eq. (20) for mixed or forced convection with 90 % confidence interval limits.

narrower the confidence interval, the higher the probability that the difference between the Sh number determined by the equation and from the measurement data will be small.

Based on the investigations, we recommend the new dimensionless Eq. (20) for calculating the evaporation rate of open-surface water with steady-state gas and liquid conditions under mixed or forced convection. Because this equation best approximated the measured Sh numbers and thus also the measured evaporation rate values, since it gave the smallest MAE, RE and RMSE, as well as the largest R^2 value. In addition, we obtained the best results for the new Eq. (20) according to the Bland-Altman method.

Thus, Fig. 7 shows the new dimensionless equation with the 90 % confidence interval and the measurement results created for the case of evaporation with steady-state gas and liquid conditions under mixed or forced convection. The upper limit of the confidence interval is +26 %, while the lower limit is -24 %. The equation gives the Sh number in the given validity range with an RE of 12.4 %.

4. Conclusion

In our previous work, a dimensionless correlation with a relative error of 9.5 % was created for evaporation under natural convection [42], where evaporation took place with steady-state gas and liquid conditions. In present publication, we have continued that work, where the study was extended to evaporation under mixed and forced convection.

Publications dealing with the evaporation of open-surface liquids under mixed and forced convection found in the literature were collected for the case of evaporation with steady-state gas and liquid conditions. During our work, our goal was to create a Sherwood equation that can be applied in a wide range of validity and gives the evaporation rate with sufficient accuracy. In addition to the Re number, the new dimensionless equation includes the Ri number, the Sc number, as well as the gas and liquid temperatures, the partial vapor pressures of the gas and the air pressure above the liquid surface.

To create the new dimensionless equation, we used measurement results found in the literature, which were published with appropriate data. Among numerous measurement results, only 8 articles provided adequate data for this, a total of 487 data sets. In addition, we carried out measurements for the evaporation of water under mixed and forced convection, at different air velocities ($v_G = 0.5 - 3.5$ m/s) and air tem-

peratures ($T_G^C = 30 - 80^\circ\text{C}$). Thus, together with the 32 data sets, own measurement results, a total of 519 measurement data sets were available. A calculation algorithm was developed for processing the measurement results. Based on the measurement data sets, the exponents and coefficients were determined in the new dimensionless equation using regression analysis. With the established dimensionless equation, the evaporation rate can be determined for the case of evaporation with steady-state gas and liquid conditions.

The new dimensionless equation was compared with the equations giving the evaporation rate with steady-state gas and liquid conditions under mixed and forced convection found in the literature. We found 28 equations that can be classified into this evaporation case. The collected measurement results were substituted into all 28 equations. However, there were equations where data were requested (e.g. air duct flow cross-section) that were not available in all 519 measurement data sets. Thus, we could only use a total of 26 equations for the comparison. Using a statistical method, we compared the new dimensionless equation with the 26 equations from the literature. Some of the equations gave strongly outlier results, these were ignored in the further investigation. Thus, a total of 17 equations were used from the original 28 equations.

Three correlations (Eq. (20), [52]/a, [1]/b) approximated the evaporation rate values from the measurement results quite well. the correlation of Moghiman and Jodat [1]/b and Raimundo et al. [52]/a gave similar values. The new equation gave the smallest deviation compared to the measured results in the examined range of $1400 \leq Re \leq 1.85 \cdot 10^5$. The results was supported by statistical indicators and the Bland-Altman method. For the new Eq. (20) dimensionless equation, the RE between the measured and calculated Sh numbers was 12.4 %. Furthermore, the R^2 of the Eq. (20) was the highest value with 0.91, while the RMSE and MAE values were also the best. The upper limit of the 90 % confidence interval is +26 %, while the lower limit is -24 %.

CRedit authorship contribution statement

Evelin VARJU: Writing – review & editing, Writing – original draft, Visualization, Validation, Software, Methodology, Investigation, Formal analysis, Data curation, Conceptualization. **Tibor POÓS:** Writing – review & editing, Supervision, Resources, Project administration, Methodology, Funding acquisition, Conceptualization.

Declaration of competing interest

The authors declare that they have no known competing financial interests or personal relationships that could have appeared to influence the work reported in this paper.

Data availability

Data will be made available on request.

Appendix

In order to carry out the dimensional analysis, it is necessary to collect the parameters influencing the investigated phenomenon, together with their dimensions. The parameters influencing the evaporation rate of the liquid in the mixed convection are shown in Table A/1.

Table A/1

The parameters influencing the evaporation rate and their basic SI units in case of mixed convection.

	Parameter	Notation	Dimension	SI unit
1	characteristic length	L_e	L	m
2	mass transfer coefficient	k_c	LT^{-1}	ms^{-1}
3	dynamic viscosity	μ_G	$ML^{-1}T^{-1}$	$kgm^{-1}s^{-1}$
4	temperature of the liquid surface	T_L^f	τ	K
5	temperature of bulk gas	T_G^G	τ	K
6	gas velocity	v_G	LT^{-1}	ms^{-1}
7	buoyancy force	$g\Delta\rho_G$	$ML^{-2}T^{-2}$	$kgm^{-2}s^{-2}$
8	diffusion coefficient	D_{LG}	L^2T^{-1}	m^2s^{-1}
9	density of gas	ρ_G	ML^{-3}	kgm^{-3}
10	total pressure of the gas	p_{tot}	$ML^{-1}T^{-2}$	$kgm^{-1}s^{-2}$
11	partial pressure difference of liquid-vapor	Δp_v	$ML^{-1}T^{-2}$	$kgm^{-1}s^{-2}$

Power product of the parameters:

$$\prod L_e^\alpha k_c^\beta \mu_G^\gamma (T_L^f)^\delta (T_G^G)^\varepsilon v_G^\theta (g\Delta\rho_G)^\pi D_{LG}^\vartheta \rho_G^\sigma p_{tot}^\varphi \Delta p_v^\omega, \quad (A1)$$

by entering the dimensions:

$$\prod [L]^\alpha [LT^{-1}]^\beta [ML^{-1}T^{-1}]^\gamma [\tau]^\delta [\tau]^\varepsilon [LT^{-1}]^\theta [ML^{-2}T^{-2}]^\pi [L^2T^{-1}]^\vartheta [ML^{-3}]^\sigma [ML^{-1}T^{-2}]^\varphi [ML^{-1}T^{-2}]^\omega \quad (A2)$$

then sorted by basic quantities:

$$\prod [L]^{\alpha+\beta-\gamma+\theta-2\pi+2\vartheta-3\sigma-\varphi-\omega} [M]^{\gamma+\pi+\sigma+\varphi+\omega} [T]^{-\beta-\gamma-\theta-2\pi-\vartheta-2\varphi-2\omega} [\tau]^{\delta+\varepsilon}. \quad (A3)$$

For \prod to be dimensionless, the sum of the components of the basic quantities must be zero:

For L:

$$\alpha + \beta - \gamma + \theta - 2\pi + 2\vartheta - 3\sigma - \varphi - \omega = 0, \quad (A4)$$

For M:

$$\gamma + \pi + \sigma + \varphi + \omega = 0, \quad (A5)$$

For T:

$$-\beta - \gamma - \theta - 2\pi - \vartheta - 2\varphi - 2\omega = 0, \quad (A6)$$

For τ :

$$\delta + \varepsilon = 0. \quad (A7)$$

Since we have 4 equations for 11 variables, the system of equations is underspecified. According to the Buckingham theorem, we can convert the original relation into a relation between 11 and 4 dimensionless power products since we have 4 basic quantities (L , M , T , τ). Of the 11 variables in the system of Eqs. (A4)-(A7), expressing the exponents (α , γ , δ , σ) of four quantities (L_e , μ_G , T_G^G , ρ_G) by the exponents of other quantities leaves only the desired six exponents (β , ε , θ , π , ϑ , φ , ω).

From τ :

$$\delta = -\varepsilon, \quad (A8)$$

From T:

$$\gamma = -\beta - \theta - 2\pi - \vartheta - 2\varphi - 2\omega, \quad (A9)$$

Acknowledgements

This work was supported by the János Bolyai Research Scholarship of the Hungarian Academy of Sciences (BO/00059/23/6) and by the Hungarian Scientific Research Fund (NKFIH FK-142204). The second author was supported by the ÚNKP-23-5-BME-411 New National Excellence Program of the Ministry for Culture and Innovation from the source of the National Research, Development and Innovation Fund.

From M:

$$\sigma = \beta + \theta + \pi + \vartheta + \varphi + \omega, \quad (\text{A10})$$

From L:

$$\alpha = \beta + \theta + 3\pi + 2\varphi + 2\omega. \quad (\text{A11})$$

This gives the new form of Eq. (A1):

$$\prod L_e^{\beta+\theta+3\pi+2\varphi+2\omega} k_c^\beta \mu_G^{-\beta-\theta-2\pi-2\varphi-2\omega} (T_L^f)^{-\varepsilon} (T_G^G)^\varepsilon v_G^\theta (g\Delta\rho_G)^\pi D_{LG}^\vartheta \rho_G^{\beta+\theta+\pi+\varphi+\omega} p_{tot}^\varphi \Delta p_v^\omega \quad (\text{A12})$$

and then sorted by exponents:

$$\prod \left(\frac{L_e k_c \rho_G}{\mu_G} \right)^\beta \left(\frac{T_G^G}{T_L^f} \right)^\varepsilon \left(\frac{L_e v_G \rho_G}{\mu_G} \right)^\theta \left(\frac{L_e^3 g \Delta \rho_G \rho_G}{\mu_G^2} \right)^\pi \left(\frac{D_{LG} \rho_G}{\mu_G} \right)^\vartheta \left(\frac{L_e^2 \rho_G p_{tot}}{\mu_G^2} \right)^\varphi \left(\frac{L_e^2 \rho_G \Delta p_v}{\mu_G^2} \right)^\omega \quad (\text{A13})$$

θ is the exponent of the Re $\left(\frac{L_e v_G \rho_G}{\mu_G} \right)$, π is the exponent of the Gr number $\left(\frac{g \Delta \rho_G L^3 \rho_G}{\mu_G^2} \right)$, ϑ is the exponent of the reciprocal of the Sc number $\left(\frac{\mu_G}{\rho_G D_G} \right)$. The product of the Gr and Sc number gives the Ra number, which characterizes the natural convection: $\left(\frac{g \Delta \rho_G L^3}{\mu_G D_G} \right)$. The quotient of the Gr number and the square of the Re number gives the Ri number, which is used to distinguish the gas flow categories: $\left(\frac{Gr}{Re^2} \right)$. ε is the exponent of the gas and liquid temperature correction term $\left(\frac{T_G^G}{T_L^f} \right)$. The Sh number is obtained as the quotient of the quantities with β and ϑ exponent $\left(\frac{k_c L}{D_G} \right)$, while the quotient of the variables ω and φ exponents gives the correction term derived from the partial pressure difference of the liquid vapor and the gas total pressure: $\left(\frac{\Delta p_v}{p_{tot}} \right)$. Thus, the use of these dimensionless quantities gives a dimensionless equation describing the phenomenon of evaporation:

$$Sh = ARi^B Re^C Sc^D \left(\frac{T_G + 273.15}{T_f + 273.15} \right)^E \left(\frac{\Delta p_v}{P} \right)^F \quad (\text{A14})$$

References

- [1] M. Moghiman, A. Jodat, Effect of air velocity on water evaporation rate in indoor swimming pools, Iran. J. Mech. Eng. 8 (2007) 19–30.
- [2] A. Jodat, M. Moghiman, M. Anbarsooz, Experimental comparison of the ability of dalton based and similarity theory correlations to predict water evaporation rate in different convection regimes, Heat Mass Transf 48 (2012) 1397–1406, <https://doi.org/10.1007/s00231-012-0984-z>.
- [3] M.M. Shah, Evaluation of available correlations for rate of evaporation from undisturbed water pools to quiet air, Int. J. HVACR Res. 8 (2002) 125–132.
- [4] M.M. Shah, Improved method for calculating evaporation from indoor water pools, Energy Build 49 (2012) 306–309, <https://doi.org/10.1016/j.enbuild.2012.02.026>.
- [5] C.C. Smith, R.W. Jones, G.O.G. Löf, Energy requirements and potential savings for heated indoor swimming pools, ASHRAE Trans 99 (1993) 864–874.
- [6] C.E. Hylgaard, Water Evaporation in Swimming Baths, Institut for Bygningsteknik, Aalborg Universitet, Oslo, 1990.
- [7] M.M. Shah, Methods for calculation of evaporation from swimming pools and other water surfaces, ASHRAE Trans 120 (2014) 3–17.
- [8] M.M. Shah, Improved model for calculation of evaporation from water pools, Sci. Technol. Built Environ. 24 (2018) 1064–1074, <https://doi.org/10.1080/23744731.2018.1483157>.
- [9] S.O. Hanssen, H.M. Mathisen, Evaporation from Swimming Pools, Proc Roomvent (1990) 1–15.
- [10] M.T. Pauken, An experimental investigation of combined turbulent free and forced evaporation, Exp. Therm. Fluid Sci. 18 (1998) 334–340, [https://doi.org/10.1016/S0894-1777\(98\)10038-9](https://doi.org/10.1016/S0894-1777(98)10038-9).
- [11] E.E. Adams, D.J. Cosler, K.R. Helfrich, Evaporation from heated water bodies: predicting combined forced plus free convection, Water Resour. Res. 26 (1990) 425–435, <https://doi.org/10.1029/WR026i003p00425>.
- [12] J. Dalton, Experimental essays on the constitution of mixed gases; on the force of steam or vapor from waters and other liquids in different temperatures, both in a torricellian vacuum and in air; on evaporation; and on the expansion of gases by heat, Mem. Proc. Manch. Lit. Philos. Soc. 5 (1802) 535–602.
- [13] G.W. Himus, J.W. Hinchley, The effect of a current of air on the rate of evaporation of water below the boiling point, J. Soc. Chem. Ind. 43 (1924) 840–845, <https://doi.org/10.1002/jctb.5000433402>.
- [14] K. Leven, Beitrag zur Frage der Wasserverdunstung (Contribution to the Question of Water Evaporation), Wärme Kältetech 44 (1942) 161–167.
- [15] K.O. Braun, K.J. Caplan, Evaporation rate of volatile liquids, pace laboratories, Minneapolis (1992). <https://ntrl.ntis.gov/NTRL/dashboard/searchResults/tit leDetail/PB92232305.xhtml>. Accessed August 13, 2018.
- [16] R. Tang, Y. Etzion, Comparative studies on the water evaporation rate from a wetted surface and that from a free water surface, Build. Environ. 39 (2004) 77–86, <https://doi.org/10.1016/j.buildenv.2003.07.007>.
- [17] M.A. Kohler, T.J. Nordenson, W.E. Fox, Evaporation from pans and lakes, US Weather Bur. Res. Pap. (1955).
- [18] H. Thiesenhusen, Untersuchungen über die Wasserverdunstungsgeschwindigkeit in Abhängigkeit von der Temperatur des Wassers, der Luftfeuchtigkeit und Windgeschwindigkeit, Gesund. Ing. 53 (1930) 113–119.
- [19] H.E. Sweers, A nomogram to estimate the heat-exchange coefficient at the air-water interface as a function of wind speed and temperature; a critical survey of some literature, J. Hydrol. 30 (1976) 375–401, [https://doi.org/10.1016/0022-1694\(76\)90120-7](https://doi.org/10.1016/0022-1694(76)90120-7).
- [20] J.J. Marciano, E.G. Harbeck, Mass-transfer studies, geological survey professional paper, U.S., 1954.
- [21] W. Brutsaert, Heat and Water Vapor Exchange Between Water Surface and Atmosphere, Office of Research and Monitoring, Washington D.C., 1973.
- [22] B.M. Smolsky, G.T. Sergeyev, Heat and mass transfer with liquid evaporation, Int. J. Heat Mass Transf. 5 (1962) 1011–1021, [https://doi.org/10.1016/0017-9310\(62\)90081-9](https://doi.org/10.1016/0017-9310(62)90081-9).
- [23] Carl. Rohwer, Evaporation from Free Water Surfaces, U.S. Dept. of Agriculture, Washington, 1931.
- [24] T. Russell, Depth of evaporation in the United States, Mon. Weather Rev. 16 (1888) 235–239.
- [25] D. Mackay, R.S. Matsugu, Evaporation rates of liquid hydrocarbon spills on land and water, Can. J. Chem. Eng. 51 (1973) 434–439, <https://doi.org/10.1002/cjce.5450510407>.
- [26] F. Heymes, L. Aprin, A. Bony, S. Forestier, S. Cirocchi, G. Dusserre, An experimental investigation of evaporation rates for different volatile organic compounds, Process Saf. Prog. 32 (2013) 193–198, <https://doi.org/10.1002/prs.11566>.
- [27] P.K. Raj, J.A. Morris, Source characterization of heavy gas dispersion models for reactive chemicals, Technol. Manag. Syst. Inc (1987).
- [28] M. Lurie, N. Michailoff, Evaporation from Free Water Surface, Ind. Eng. Chem. 28 (1936) 344–349.
- [29] J. Chen, C. Chen, Uncertainty analysis in humidity measurements by the psychrometer method, Sensors 17 (2017) 368, <https://doi.org/10.3390/s17020368>.
- [30] M. Al-Shammiri, Evaporation rate as a function of water salinity, Desalination 150 (2002) 189–203, [https://doi.org/10.1016/S0011-9164\(02\)00943-8](https://doi.org/10.1016/S0011-9164(02)00943-8).
- [31] A.F. Meyer, Evaporation from Lakes and Reservoirs, Minnesota Resources Commission, St. Paul, Minn., 1942.
- [32] R.E. Horton, A new evaporation formula developed. empirical statement based on physical laws agrees with observed facts and is held to be an improvement over existing formulas, Eng. News-Rec. 78 (1917) 196–199.
- [33] J.W. Finch, R.L. Hall, Estimation of Open Water Evaporation, Environment Agency, 2001.
- [34] M.A. Kohler, Lake and Pan Evaporation, Geological Survey Professional Paper, U. S., 1954.

- [35] M.A. Kohler, T.J. Nordenson, W.E. Fox, Pan and Lake Evaporation, Geological Survey Professional Paper, U.S., 1958.
- [36] M. Haji, L.C. Chow, Experimental measurement of water evaporation rates into air and superheated steam, *J. Heat Transf.* 110 (1988) 237–242, <https://doi.org/10.1115/1.3250457>.
- [37] R.W. Powell, Evaporation of water from saturated surfaces I, *Engineering* 150 (1940) 238–239.
- [38] W. Brutsaert, S.L. Yu, Mass transfer aspects of pan evaporation, *J. Appl. Meteorol.* 7 (1968) 563–566, [https://doi.org/10.1175/1520-0450\(1968\)007<0563:MTAOPE>2.0.CO;2](https://doi.org/10.1175/1520-0450(1968)007<0563:MTAOPE>2.0.CO;2).
- [39] A.A. Hummel, K.O. Braun, M.C. Fehrenbacher, Evaporation of a liquid in a flowing airstream, *Am. Ind. Hyg. Assoc. J.* 57 (1996) 519–525, <https://doi.org/10.1080/15428119691014729>.
- [40] W.J. Shuttleworth, *Evaporation, Handb. Hydrol.* (1993).
- [41] E.G. Harbeck, A practical field technique for measuring reservoir evaporation utilizing mass-transfer theory, Washington, 1962.
- [42] E. Varju, T. Poós, New dimensionless correlation for mass transfer at evaporation of open liquid surface in natural convection, *Int. Commun. Heat Mass Transf.* 136 (2022) 106102, <https://doi.org/10.1016/j.icheatmasstransfer.2022.106102>.
- [43] K. Biasin, W. Krumme, Die Wasserverdunstung in einem Innenschwimmbad (Water Evaporation in an Indoor Swimming Pool), *Electrowärme Int* 32 (1974) A115–A129.
- [44] Y.-C. Yen, G.R. Landvatter, Evaporation of Water into a Sub-Zero Air Stream, *Water Resour. Res.* 6 (1970) 430–439, <https://doi.org/10.1029/WR006i002p00430>.
- [45] V.V. Baturin, *Fundamentals of Industrial Ventilation*, Pergamon Press, New York, 1972.
- [46] C.O. Bennett, J.E. Myers, *Momentum, heat, and Mass Transfer*, McGraw-Hill, New York, 1974, 2nd ed, <http://trove.nla.gov.au/version/44867893>. Accessed October 13, 2017.
- [47] W. Chuck, E.M. Sparrow, Evaporative mass transfer in turbulent forced convection duct flows, *Int. J. Heat Mass Transf.* 30 (1987) 215–222, [https://doi.org/10.1016/0017-9310\(87\)90109-8](https://doi.org/10.1016/0017-9310(87)90109-8).
- [48] E. Sartori, A mathematical model for predicting heat and mass transfer from a free water surface, *Adv. Sol. Energy Technol.* 4 (1988) 3160–3164.
- [49] A. Rotkegel, An Experimental Study of Counterdiffusional Nonequimolar Mass Transfer in Nonisothermal Multicomponent Systems, Institute of Chemical Engineering, Polish Academy of Science, 1995.
- [50] R. Krupiczka, A. Rotkegel, An experimental study of diffusional cross-effects in multicomponent mass transfer, *Chem. Eng. Sci.* (1997). <https://www.semanticscholar.org/paper/An-experimental-study-of-diffusional-cross-effects-Krupiczka-Rotkegel/bbcb551074c83306160846ed942a0a4103e70ca6>. Accessed November 2, 2021.
- [51] C. Yanagi, M. Murase, Y. Yoshida, T. Iwaki, T. Nagae, Y. Koizumi, Evaporation heat flux from hot water to air flow, *Trans. Jpn. Soc. Mech. Eng. Ser. B* 78 (2012) 363–372, <https://doi.org/10.1299/kikaib.78.363>.
- [52] A.M. Raimundo, A.R. Gaspar, A.V.M. Oliveira, D.A. Quintela, Wind tunnel measurements and numerical simulations of water evaporation in forced convection airflow, *Int. J. Therm. Sci.* 86 (2014) 28–40, <https://doi.org/10.1016/j.ijthermalsci.2014.06.026>.
- [53] M. Inan, Ş.O. Atayilmaz, Experimental investigation of evaporation from a horizontal free water surface, *Sigma J. Eng. Nat. Sci.* 35 (2017) 119–131.
- [54] E. Varju, Atmospheric Evaporation of open, Still Water Surface Under Steady-State Conditions, Budapest University of Technology and Economics, 2023. <https://repozitorium.omikk.bme.hu/handle/10890/41828>.
- [55] P.T. Tsilingiris, Review and critical comparative evaluation of moist air thermophysical properties at the temperature range between 0 and 100°C for Engineering Calculations, *Renew. Sustain. Energy Rev.* 83 (2018) 50–63, <https://doi.org/10.1016/j.rser.2017.10.072>.
- [56] Vapor Pressure Calculation by Antoine Equation (Water), (n.d.). <http://ddbonline.ddbst.de/AntoineCalculation/AntoineCalculationCGL.exe?component=Water> (accessed February 26, 2021).
- [57] W.L. McCabe, J.C. Smith, P. Harriott, *Unit Operations in Chemical Engineering*, McGraw-Hill Inc., US, New York, 1993, 5th Revised edition edition.
- [58] Apollo application, (n.d.). https://www.interconnect.hu/index2_hu.php (accessed March 13, 2023).
- [59] J.L. Devore, *Devore Probability Statistics Engineering Sciences*, 8th ed., Brooks/Cole, Boston, n.d.
- [60] M. Horváth, T. Csoknyai, Evaluation of solar energy calculation methods for 45° inclined, South facing surface, *Energy Procedia* 78 (2015) 465–470, <https://doi.org/10.1016/j.egypro.2015.11.700>.
- [61] M.T.C. | A.H. Company, Air pressure at altitude calculator, (n.d.). <https://www.mide.com/air-pressure-at-altitude-calculator> (accessed January 3, 2023).
- [62] J.L.F. Blázquez, I.R. Maestre, F.J.G. Gallero, P.Á. Gómez, Experimental test for the estimation of the evaporation rate in indoor swimming pools: validation of a new CFD-based simulation methodology, *Build. Environ.* 138 (2018) 293–299, <https://doi.org/10.1016/j.buildenv.2018.05.008>.
- [63] F. Asdrubali, A scale model to evaluate water evaporation from indoor swimming pools, *Energy Build* 41 (2009) 311–319, <https://doi.org/10.1016/j.enbuild.2008.10.001>.
- [64] F.J.G. Gallero, I.R. Maestre, J.L. Foncubierta Blázquez, J.D. Mena Baladés, Enhanced CFD-based approach to calculate the evaporation rate in swimming pools, *Sci. Technol. Built Environ.* 27 (2021) 524–532, <https://doi.org/10.1080/23744731.2020.1868219>.
- [65] B.R. Hugo, Modeling Evaporation from Spent Nuclear Fuel Storage Pools: A Diffusion Approach, PhD Thesis, Washington State University, 2015.
- [66] E.K. Webb, An Investigation of the Evaporation from Lake Eucumbene, Commonwealth Scientific and Industrial Research Organization, Melbourne, Australia, 1960.
- [67] F.H. Bigelow, Studies on the phenomena of the evaporation of water over lakes and reservoirs II, *Mon. Weather Rev.* 36 (1908) 24–39.
- [68] F.H. Bigelow, Studies on the phenomena of the evaporation of water over lakes and reservoirs III, *Mon. Weather Rev.* 36 (1908) 437–445.
- [69] J.M. Bland, D.G. Altman, Statistical methods for assessing agreement between two methods of clinical measurement, *Lancet Lond. Engl.* 1 (1986) 307–310.